Protection of concrete slabs with granular material against explosive actions: Experimentation and modelling

Ricardo Ramos

November 2017

Abstract

Nowadays, the catastrophic effects of explosive actions by terrorist groups have been observed on a large scale. Consequently, the damage caused has alarmed international security and has caused a climate of instability in populations. There is an urgency to focus on the protection of critical infrastructures, which are valuable for many reasons. This work, based by Ramos (2017), aims to analyse the contribution of granular materials to the protection of structural elements subject to explosions.

In this study, slabs represented the structural elements to be protected. The protection was materialized through reno mattresses filled with the granular material. An experimental campaign was carried out, where it was tested: a reference slab and two slabs covered with the protection solution. Also, a finite element model was also constructed in order to simulate the experimental conditions and to integrate relevant knowledge.

Considering the results obtained in this work, it was concluded that the granular material is an appropriate solution for the protection of structural elements. However, the protection is limited by a maximum value of thickness.

Keywords: Explosive actions, granular materials, protection, reno mattress, experimental campaign.

1 Introduction

In the last decades, terrorist organizations use the IED threat to generate chaos in large population centers. It is extremely important to improve infrastructures able to resist the effects of these explosive events. Thus, it is of great importance the engineering development to improve the structural behaviour of critical buildings affected to explosive actions. However, it is not allowed to perform structural intervention on most of the buildings in city centres. Thus, it is intended to analyse a reinforcing solution to structural elements which reduces explosive damages.

The protective solution studied consists in a reno mattress filled with granular material. The main objective is to understand if this solution has the capacity to reduce the blast effects on structural elements present in roofs.

A very relevant phase of this study is the planning and carrying out of explosive tests on materials considered. It is intended the realization of a numerical model that allows to simulate the conditions of the present study. This numerical model will have the advantage of running an unlimited number of analysis of different physical parameters. It will be also studied analytical approaches from the UFC 3-340-02 (2008) and from another authors to understand the action and the response of the materials.

2 Blast load

2.1 The load

An explosive action is an extremely rapid reaction (on the order of milliseconds), which results in an instantaneous release of energy and gases at high temperatures (Karlos e Solomon 2013).

2.2 Blast wave

In order to evaluate the blast wave as a function of the pressure and time, the free air burst model (radially propagation wave) is assumed. As shown in Figure 2.1, after detonation the formed shock wave takes t_a (arrival time of shock wave) to reach a certain point. At this time, the pressure increases from P_0 (ambient pressure) to P_{S0} (peak incident pressure). During positive pressure, i_S^+(incident impulse) is important to quantify damages. Then the overpressure will decrease during t_d (duration of the positive phase) until reaches P_{min} (minimum pressure of blast), which is the peak of a negative phase, manifested as a suction (Wilkinson & Anderson 2003).

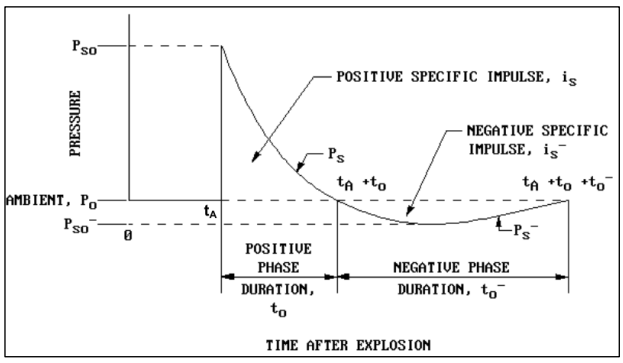

Figure 2.1 Pressure-time of air burst (UFC 3-340-02 (2008)

Friedlander suggests equation (2.1), that represents pressure-time of blast wave phenomena (Guzas & Earls, 2010)

$$P(t) = \begin{cases} 0, & t < t_a, \\ P_{S0}\left(1 - \dfrac{t - t_a}{t_d}\right) e^{-b\left(\frac{t-t_a}{t_d}\right)}, & t_a \le t \le t_a + t_d, \\ 0, & t > t_a + t_d, \end{cases} \quad (2.1)$$

Where b is the decay constant.

2.3 Quantification of blast load

Although being different types of explosives. It is important to convert different effects into a reference unit. Equation (2.2) shows a TNT equivalency based on heat of detonation (Wilkinson & Anderson 2003).

$$W_E = \frac{H_{EXP}^d}{H_{TNT}^d} W_{EXP} \quad (2.2)$$

Where W_E is effective charge weight, W_{EXP} is weight of explosive in question, H_{EXP}^d = Heat of detonation of explosive in question and H_{TNT}^d = Heat of detonation of TNT.

Hopkinson states that when two charges with the same explosive are detonated in the same atmospheric conditions, the effects of shock waves are similar. That is, if they are arranged at a scaled distance, Z (equation (2.3)).

$$Z = \frac{R}{\sqrt[3]{W}} [m/Kg^{1/3}] \quad (2.3)$$

Where R is the distance to the detonation source and W is the mass of the explosive charge.

The incident peak pressure is a very important parameter in the evaluation of the effects of the explosive action. Kinney & Graham (1985) suggests equation (2.4) to calculate incident peak pressure.

$$P_{S0} = 808 P_0 \frac{\left[1 + (\frac{Z}{4,5})^2\right]}{\sqrt{\left[1 + (\frac{Z}{0,048})^2\right]\left[1 + (\frac{Z}{0,32})^2\right]\left[1 + (\frac{Z}{1,35})^2\right]}} \text{ [bar]} \quad (2.4)$$

2.4 Surface interaction

If the shock wave finds an obstacle that offers resistance the response will be a reflection. As illustrated on Figure 2.2, α (angle of incidence) will define the type of reflection. Karlos & Solomon (2013) refer that the situation with greater damage is when $\alpha = 0^\circ$ - normal reflection.

If the incident wave intercepts the reflected wave in a triple point, it will be originated a Mach stem. As suggests Figure 2.2, the height of the front Mach increases with the increase of the propagation distance.

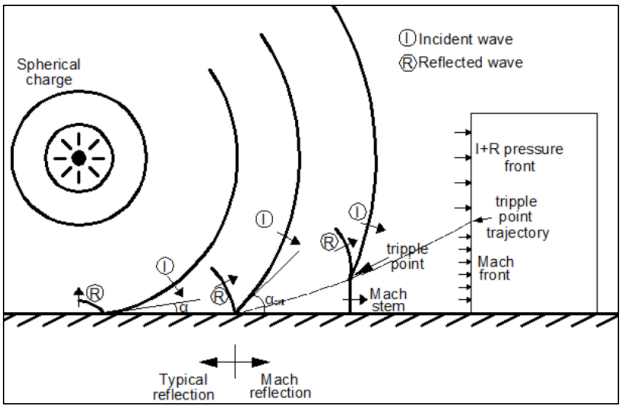

*Figure 2.2 Influence of surface on the propagation of shock waves ((*Karlos & Solomon 2013)

Equation (2.5), proposed by Needham (2010), estimates peak reflected pressure (P_{R0}) in function of P_{S0}.

$$P_{R0} = 2P_{S0} \frac{4P_{S0} + 7P_0}{4P_{S0} + 7P_0} \text{ [MPa]} \quad (2.5)$$

3 Response of materials to blast load

3.1 Materials

3.1.1 Soil

Soil can be admitted with an elastic and plastic behaviour and a Mohr-Coulomb criterion. The Mohr-Coulomb criterion establishes that the resistance of soil increases proportionally to normal stress. The failure occurs when the line defined by (3.1) is tangent to Mohr´s circle (Stromblad, 2014).

$$\tau_f = c' + \sigma'_{nf} \cdot \tan\varphi' \quad (3.1)$$

Where τ_f is the tangential stress, σ'_n is the normal stress, c' is the cohesion and φ' is the friction angle.

An et al. (2011) refers that a dry soil under a dynamic load has different behaviours. At low pressures that are elastic deformations on bonds in contact with the surface of particles. Increasing pressure, there is a failure in the bond and, consequently, displacements of particles. Increasing applied pressure further, all soil components are deformed. Wang et al. (2004) state that in a blast load, the reduced duration of the phenomenon does not allow air and water to circulate through the solid skeleton. There is a simultaneous response of three components (mineral matter, water and air).

3.1.2 Reinforced concrete

Magnusson (2007) relates that under a blast load reinforced concrete reach higher values of tension than a static load. A dynamic increase factor (DIF) is applied materials to quantify the difference between dynamic and static behaviour. Ngo et al. (2007) stated equation (*3.2*) to characterize DIF in function of strain rates.

$$\mathrm{DIF} = \begin{cases} \dfrac{f_{c,din}}{f_c} = \left(\dfrac{\dot{\varepsilon}}{\dot{\varepsilon}_s}\right)^{1.026\alpha}, & \dot{\varepsilon} \le \dot{\varepsilon}_1 \\ \dfrac{f_{c,din}}{f_c} = A_1 \ln(\dot{\varepsilon}_1) - A_2, & \dot{\varepsilon} > \dot{\varepsilon}_1 \end{cases} \quad (3.2)$$

Where $f_{c,din}$ is dynamic design stress, f_c is concrete compressive strength, $\dot{\varepsilon}$ is strain rates ($30x10^{-6}$ s $^{-1}$ to 300 s $^{-1}$), $\dot{\varepsilon_s}$ is strain rates ($30x10^{-6}$ s $^{-1}$), $A_1 = -0{,}0044 f_c + 0{,}9866$ and $A_2 = -0{,}0128 f_c + 2{,}1396$ and $\alpha_s = 1/(20+f_c/2)$.

3.1.3 Protective System

In order to mitigate effects of an explosive event, must be established protective measures. UFC 3-340-02 (2008) emphasized the measure of design structures that protect the receiver system from damaged caused by donor system (Figure 3.1). Measures solution can be shelters or barriers. Barriers c

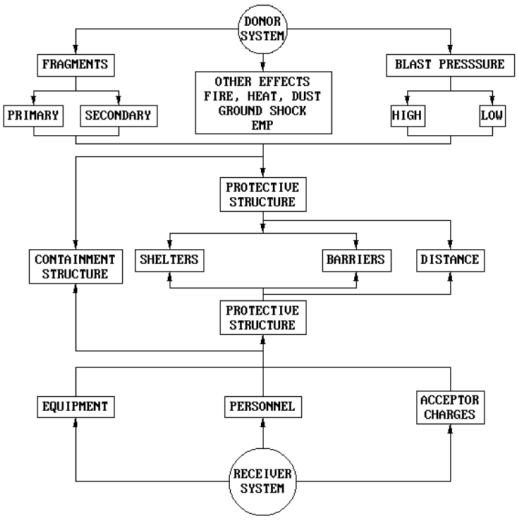

Figure 3.1 Explosive protective system (UFC 3-340-02 2008)

4 Experimental tests

4.1 Material composition and mechanical properties

4.1.1 Slabs

All slabs present in the tests have the following dimensions: 2,6 x 2,0 x 0,12 [m]. The lower mesh was ø10 // 0.20 with A500NR steel, an upper mesh was ø5 // 0.15 with A500ER steel. The concrete type C30 / 37 was used in all slabs.

In order to evaluate the compressive strength of concrete it was carried out uniaxial compression tests. 12 cubes of 150 mm were submitted to a hydraulic pressure testing. Finally, it was possible to obtain a compressive mean strength of $42{,}52$ MPa.

For reinforced concrete, it was considered a density, $d = 25\mathrm{kN/m^3}$.

4.1.2 Protective system

As represented in Figure 4.1, reno mattress has a parallelepipedal geometry with the following dimensions: 2,6 (C) x 2,0 (L) x H [m], where H defines the thickness of protective system. Dimensions of the mesh are 60 (a) x 80 (b) [mm]. To achieve an adequate productivity, it was required 2 to 3 people to build the base of the mattress.

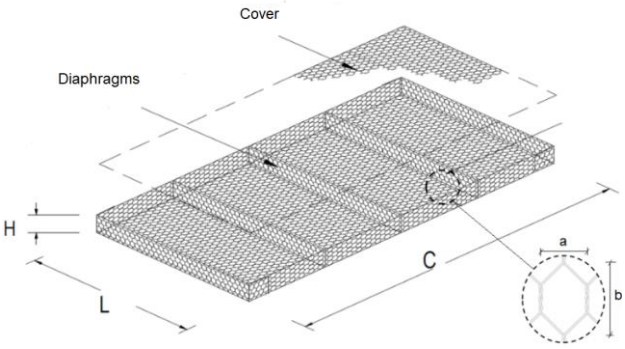

Figure 4.1 Scheme of reno mattress

The reno mattress wire has a tensile strength in the range of 380 – 560 [MPa] and it´s covered with Galfan to provide an adequate corrosion protection.

The granular material adopted to fill the reno mattress was pebble. Pebble used in experimental tests comprised a granulometric range between 20 mm and 120 mm. In order to determinate density of aggregate, it was weighed 3 vessels with the same volume. It was obtained a mean value of density, $\mathrm{d} = 1567{,}58\ [\mathrm{kg/m^3}]$.

4.1.3 Explosive charge

Commercial explosive Eurodyn ™ 2000 was used during the experimental trials. The explosive charge had a

cylindrical configuration and weighed 6 kg. Considering equation (2.2), it was obtained $W_E = 5{,}94\ \text{kg TNT}$.

4.2 Test System

As shown in figure Figure 4.2 (a), the test system consists in a metal profile that suspends the explosive charge. The explosive charge is suspended at 2m (between the geometric centre of the load and the upper face of the slab). Explosive charge is immobilized by cords to stay plant-centred with the slab and to resist wind actions. The slab is supported on "T" type beams.

A mechanical system was used due to the lack of sensors capable of withstanding explosive effects. As shown in Figure 4.2 (c), it was used 10 stems to measure initial displacements and maximum displacements.

To measure final displacements of slab after occurred explosive action, it was used a metal ruler on top of slab in positions a), b), c) (Figure 4.2) A ruler was also used to measure the thicknesses of cracks opened on the slab.

(a) Test system before charge detonation

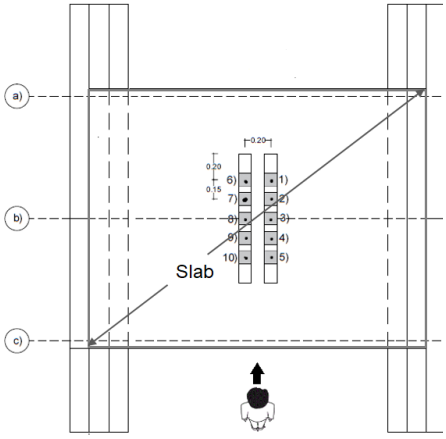

(b) Test Scheme

(c) Monitoring system based on stems

Figure 4.2 Testing and monitoring systems

4.3 Results

4.3.1 Slab without protective system (reference)

Slab without protection was constituted as reference for the remaining tests. Therefore, the effects of impact of the shock wave would serve as a basis of comparison for the other slabs with protection. It was not verified any deformation before the explosion.

As shown in Figure 4.3 (a), flexure cracks can be observed, where the orientation leads to conclude a cylindrical bending of the slab. It was also verified that most of the cracks were concentrated in mid-span of slab.

Using 8 of the 10 stems it was possible to obtain during explosive action a mean value of maximum deformation, $d = 28{,}5\ \text{mm}$ (Figure 4.3). After the slab had been subjected to the explosive action, the mean final deformation observed was 4.33 mm. This value of final deformation leads to the conclude that the slab had an elastic behaviour and remained at the level of plastic behaviour.

(a) Cracks in lower face

(b) Measurement of cracks in the edge

Figure 4.3 Resuts of slab without protection

Table 4.1 Test Results of slab without protection

Maximum Cracking [mm]		Initial displacements (mean) [mm]	Final displacements (mean) [mm]	Maximum displacements (mean) [mm]
Edge	Lower Face	Not detected	4,33	28,5
0,25	0,25			

4.3.2 Slab with protective system ($e = 0,16\ m$)

Since the unprotected slab damages were moderate, it is intended to add the protective system in order to reduce deformation. The overlapping of the mattress with the slab caused the change of the stand-off (distance between the explosive source and the upper face). However, the distance between the explosive source and the structural element to be protected remains the same.

Before the explosive action was deployed, it was possible to evaluate deformations because the slab was more requested due to the overload of the weight of the pebble. Thus, it was verified an initial displacement of $4{,}5\ \mathrm{mm}$.

Figure 4.4 (b) shows several cracks formed in the medium of slab due to blast load. The maximum size was w_k= 0,1 mm. Confronting with maximum value obtained in the reference slab, there is a 60% decrease in the thickness of the cracks. The cracking present in the lower face of the slab (Figure 4.4 (a)) had as maximum thickness of w_k= 0,15. Comparing with the values observed in the reference slab, maximum thickness decreased 40%.

During the explosive event, 9 of the 10 metal stems allowed a maximum deformation average of 18.9 mm. Compared with the first test, there was a maximum arrow decrease of 33%. After explosion event, it was possible to measure residual displacements of $4{,}67\ \mathrm{mm}$. Crossing the test of the slab without protection, there is an increase of 7% of the mean value of medium displacements.

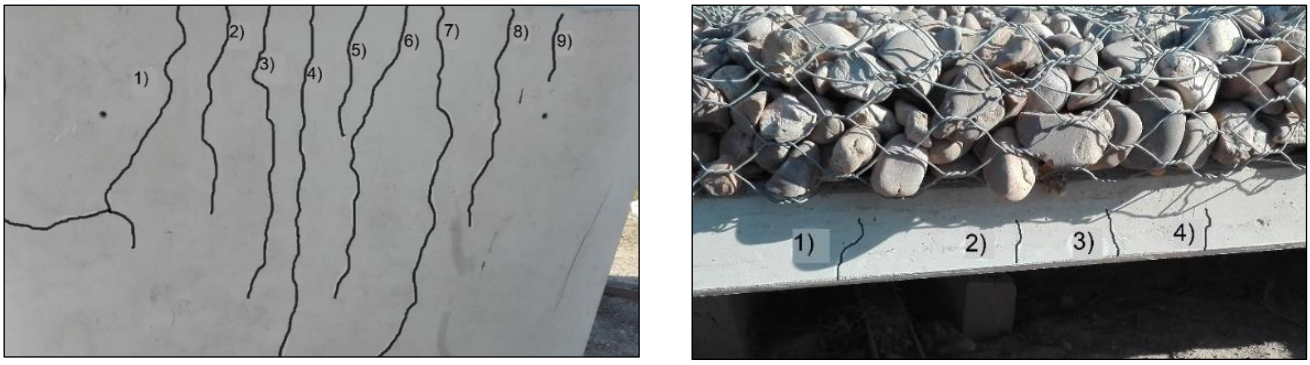

(a) Cracks in lower face (b) Measurement of cracks in the edge

Figure 4.4 Resuts of slab with protective system ($e = 0{,}16\ m$)

Table 4.2 Test Results of slab protective system ($e = 0{,}16\ m$

Maximum Cracking [mm]		Initial displacements (mean) [mm]	Final displacements (mean) [mm]	Maximum displacements (mean) [mm]
Edge	Lower Face	4,5	4,67	18,9
0,10	0,15			

4.3.3 Slab with protective system ($e = 0,22\ m$)

Again, moderate damage was noted on the slab. In this way, the protection thickness was increased to $\mathrm{e} = 0{,}22\ \mathrm{m}$. Before the explosive action was triggered the residual displacements took the mean value of 6.3 mm (Table 4.3). That is an increase of 33% over the previous test.

As result of the explosive action, there were 6 cracks located in the centre of the slab (Figure 4.5 (b)), of which, cracks marked "4" and "5)" had a higher thickness. Comparing with the results of the reference slab, there was a 20% decrease in the thickness of the cracks. In the lower face of the slab, there was a great concentration of cracks in the middle of the slab (Figure 4.5(a)). The maximum

value observed was w_k= 0,2 mm, corresponding to a decrease of 20% in reference slab.

During the explosive action, the maximum displacement registered in the slab was the mean value of 23.5 mm.

Decreased 18% when compared to the values obtained in the reference slab. After explosive event, the slab became permanently deformed with final displacement of $7\ \mathrm{mm}$.

(a) Cracks in lower face

(b) Measurement of cracks in the edge

Figure 4.5 Test Results of slab protective system ($e = 0{,}22\ m$)

Table 4.3 Test Results of slab protective system ($e = 0{,}22\ m$)

Maximum Cracking [mm]		Initial displacements (mean) [mm]	Final displacements (mean) [mm]	Maximum displacements (mean) [mm]
Edge	Lower Face	6,3	7	23,5
0,20	0,20			

4.3.4 Discussion of the results obtained in the three tests

Firstly, when comparing the results of the first two tests, it was concluded that the reno and pebble mattress set has the ability to mitigate effects resulting from the explosive action.

Taking into account the results of the third test (with protective system ($e = 0{,}22\ m$)), the increase in thickness will inevitably condition the strength of the structural element, because pebble applies a considerable overload. Thus, it is not justified to adopt a very thick mattress filled with pebble. It also be noted that good compaction has been ensured, however, the considerable dimensions of the aggregate allow the presence of voids between them. This discontinuity between the physical (aggregate) and gaseous (void) may have affected the propagation of the shock wave

5 Numerical model

5.1 Numerical model of blast load

To better understand the blast load distribution and also the behaviour of slabs under free air burst, numerical models are established in software Abaqus to reproduce field blast tests.

Abaqus uses a Conventional Weapon (ConWep) to describe blast load (pressure-time).

It´s important to understand output of ConWep. Results of analytic models of reference authors were compared with various simulations in Abaqus. it was observed that for $Z < 1$ the Abaqus provides pressure values, which in the great majority are means of the values obtained in the analytical models. However, for values of $Z > 1$, it was verified that the discrete point representation of the numerical model assumes higher pressure values than most analytical models.

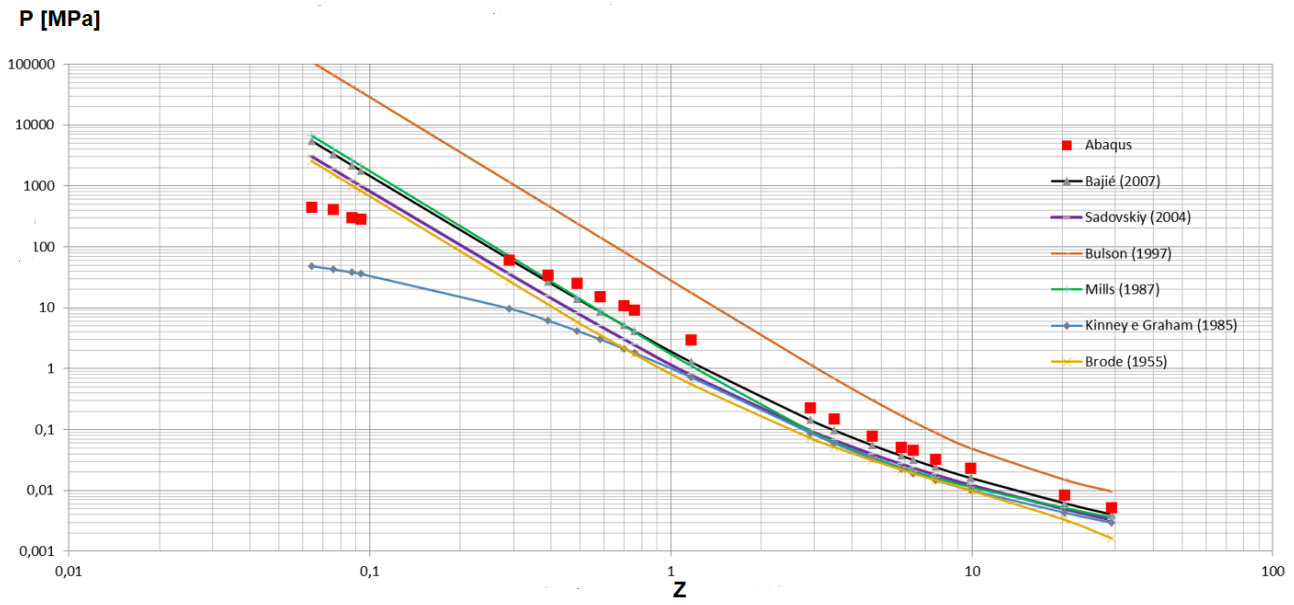

Figure 5.1 Blast load model: comparison of analytical models with Abaqus

5.2 Reinforced concrete model

In the present study, the slab is modelled admitting a homogeneous section. The shell element (S4R) is associated to the reinforced concrete section. For reinforced concrete is considered a density, $\rho = 25\ \mathrm{kN/m^3}$. Taking the equation (3.2) into account, it was obtained a DIF = 1.4. Finally, concrete compressive strength is $f_{c,din} = 60\ \mathrm{MPa}$. It was also adopted a young modulus, $E_{cm} = 32{,}73\ \mathrm{GPa}$. Using only 1 element with forces applied in the nodes, it was possible to understand by the results that the adopted constitutive model was validated with success.

5.3 Reinforced mattress and granular material element

It was assumed that in the present study the reno mattress and the granular material should be modelled as a continuous, homogeneous and isotropic. A hexagonal solid element (C3D8R) was considered. In Abaqus, it´s introduced a density $\rho = 1568\ \mathrm{kg/m^3}$. Based on Lin et al. (2000), it was assumed results of a unconfined gabion submitted to compressive test. It was possible to obtain an Young modulus, $E = 4{,}535\ \mathrm{MPa}$. A Poisson coefficient $\nu = 0{,}3$ was assumed. According to Mohr-Coulomb criteria, parameters adopted were: friction angle, $\varphi' = 35°$; Dilatancy, $\psi' = 0$ and cohesion $c' = 20\ [\mathrm{kPa}]$. Again, it was verified that constitutive model was correctly validated.

5.4 Response of the reference slab model to explosive load

Once the mechanical properties of the materials and the blast load have been validated, the model was assembled. In this way, the following option were taken in the pre-processing phase:

- On model, it´s adopted as dimensions: 2,45 x 2,00 [m]. Note by Figure 5.2 that in initial direction of the slab is removed 0.15 m from the width of the T-beam;
- In ConWep model it´s admitted an explosive charge W=5,94kg TNT, to simulate the field blast tests and W=30kg TNT to explore the plastic behaviour of slab. Both charges were distanced 2 m from slab;
- 300 steps in time along 1 s were adopted;
- Through a sensitivity analysis, it was verified that the most adequate mesh was constituted by 2080 elements;
- The following boundary conditions were admitted on edges with 2.0m: $U_X = U_Y = U_Z = UR_X = 0$ (Figure 5.2).

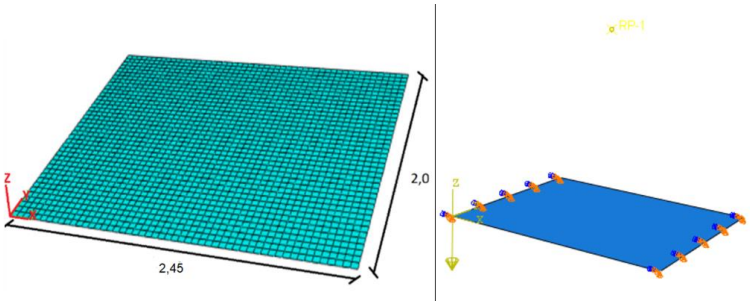

Figure 5.2 Numerical model of blast against blast load

In the first simulations, it was verified that the slab was free of damping. Rayleigh damping is allowed because it is computationally efficient.

$$C = \alpha \cdot M + \beta \cdot K \tag{5.1}$$

Where M is total mass of the element [kg], K is total element stiffness [N/m], α is a constant calculated by expression (5.2) and β is a constant calculated by expression (5.3).

$$\alpha = \frac{2 \cdot \omega_1 \cdot \omega_2 \cdot (\omega_2 \cdot \xi_1 - \omega_1 \cdot \xi_2)}{(\omega_2^2 - \omega_1^2)} \ [s^{-1}] \tag{5.2}$$

$$\beta = \frac{2 \cdot (\omega_2 \cdot \xi_2 - \omega_1 \cdot \xi_1)}{(\omega_2^2 - \omega_1^2)} \ [s^{-1}] \tag{5.3}$$

Where ξ is viscous damping coefficient and ω is natural frequency. Taking into account the equations previously mentioned, it was possible to determine a value of. $\alpha = 12{,}355$ and $\beta = 0{,}000178$

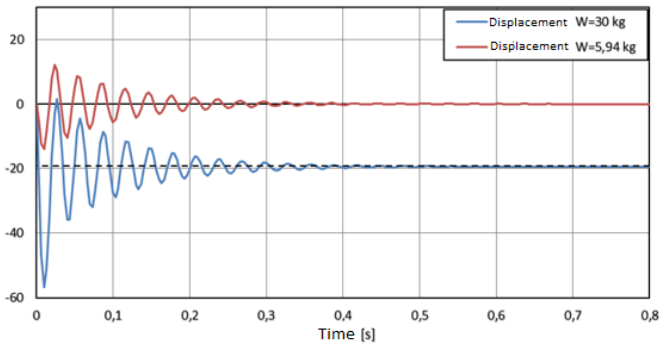

Figure 5.4 Displacement of the reference slab for: W = 5.94kg and W = 30kg

5.5 Response of the reference slab model to explosive load

As presented in Figure 5.4, the reference slab was subjected to different explosives load simulations in Abaqus: $W = 5{,}94$ kg TNT (represents explosive charge used in tests) and $W = 30$ kg TNT (used to explore plastic behaviour of slab). For the amount of explosive charge, W = 30 kg, it´s generated an higher residual displacement of 19 mm, when compared with W = 5.94 kg (0,01 mm). The increased of explosive charge allowed the slab to increase the plastic behaviour. In Figure 5.3, it is possible to verify a higher concentration of tensions in the mid-span of the slab. Where is reached the yield tension limit. For charge considered in tests, there is a maximum displacement of 17,8 mm

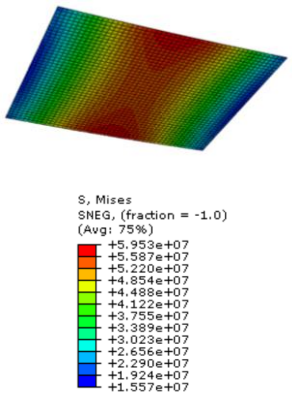

Figure 5.3 Stress levels in reference slab

5.6 Response of the slab model with protective system

The high granulometric interval and irregular pebble geometry, create difficulties in the modelling process. The different composition of granular material and reno mattress is assumed to be homogenous in model. The following thicknesses are considered for the protection of the slab: 0,16 m and 0,22m. It was verified that the addition of the protective layer in the numerical model considerably increased the processing time of Abaqus. It should be noted that, the inclusion of the protection, contained S4R elements of the slab, plus C3D8R elements of the

protection layer, totalling a maximum of 8580 finite elements. It is also emphasized that the inclusion of a

protection will change the stand-off (distance between the explosive source and the first face in contact with the explosive wave).

For a thickness of 0.16 m, there is a maximum displacement of 10,8 mm in the mid span of slab (Figure 5.6). The Figure 5.5, shows a stress concentration in the mid span region of slab.

For a thickness of 0.22 m, it´s verified a maximum displacement of 13,6 mm. Thus, the increased thickness of protection, caused an increase of deformations in the slab.

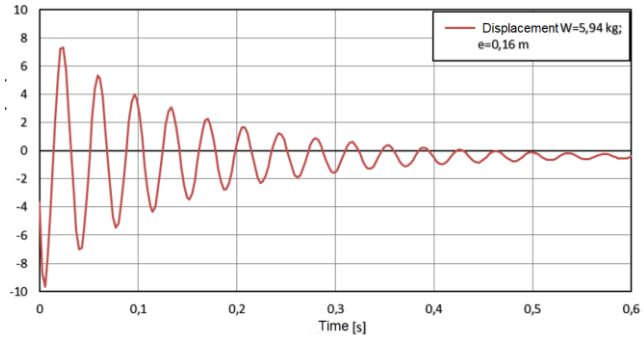

Figure 5.6 Displacement of slab with protection e=0,16 m

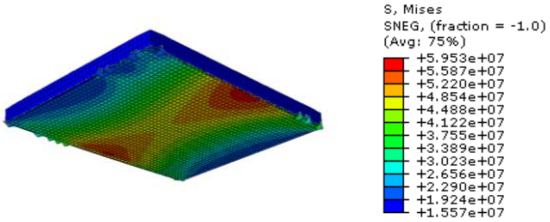

Figure 5.5 Stress levels in slab with protection e=0,16 m

5.7 Comparison of different slabs

In Figure 5.7, the initial displacements measured in the tests and obtained in the numerical model are compared. As can be seen, in all the slabs considered, the values measured in the tests are significantly higher than those obtained in the numerical model. There is also an increase of displacements proportional to the increase of protection thickness. Thus, before the blast wave being formed, deformations already exist on the slab due to the considerable density of the granular material.

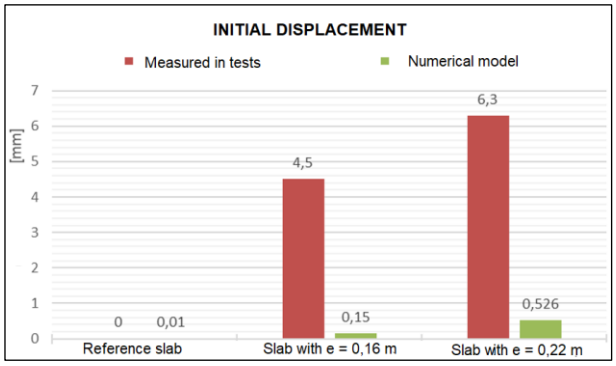

Figure 5.7 Comparison of initial deformations

Firstly, the reference slab shows a considerable difference of maximum values of deformation, which are reported to the assumptions taken in the definition of the slab model (Figure 5.8). It is also shown, in Figure 5.8, that the results obtained by the analytical approach, presents values of maximum deformation of tests larger than the tests and numerical model

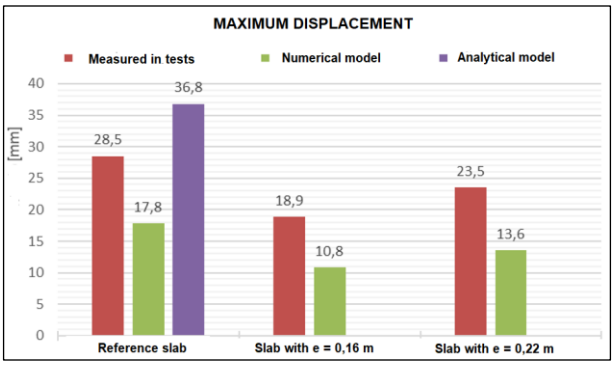

Figure 5.8 Comparison of maximum deformations

Figure 5.9 shows the values of the final deformations in the slab, obtained in the tests and in the numerical model. Comparing with the results of the initial deformations, indicated in Figure 5.9, it is noted, the increase of deformations caused by the propagation of the shock wave in the structural element.

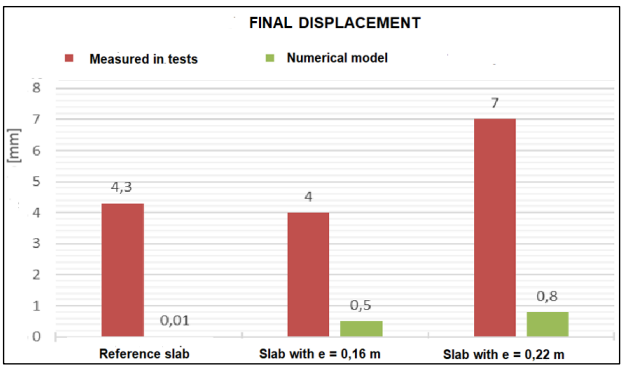

Figure 5.9 Comparison of final deformations

6 Final considerations

From the study developed, it was concluded that the application of protective system, based by granular material and reno mattress, provides a good protection. Nevertheless, in structural elements, as for example in the slabs, the application is limited. This is because, with increasing protection thickness, the weight applied by the granular material is also increased. Consequently, the slab strength decreases. Thus, for this type of structures, it is suggested to integrate a protection thickness between 0,1 m and 0,13 m. The protection solution of the present work presents the following advantages: reduced installation time; easy acquisition of materials and if necessary, it´s flexible to be changed,

References

An, J. et al., 2011. Simulation of Soil Behavior under Blast Loading. *International Journal of Geomechanics*, 11(4), pp.323–334.

Karlos, V. & Solomon, G., 2013. *Calculation of blast loads for application to structural components*,

Kinney, G. & Graham, K., 1985. *Explosive Shocks in Air*,

Lin, D., Huang, B. & Lin, S., 2000. DEFORMATION ANALYSES OF GABION STRUCTURES.

Magnusson, J., 2007. *Structural Concrete Elements Subjected to Air Blast Loading*, Stockholm.

Needham, C.E., 2010. *Blast Waves*,

Ngo, T. et al., 2007. Blast loading and blast effects on structures - An overview. *Electronic Journal of Structural Engineering*, 7, pp.76–91.

Ramos, R., 2017. *Proteção de laje de betão com material granular face a ações explosivas: Ensaio experimental e modelação*. Academia Militar/Instituto Superior Técnico.

Stromblad, N., 2014. *Modeling of Soil and Structure Interaction Subsea*.

UFC 3-340-02, 2008. *Structures to Resist the Effects of Accidental Explosions*,

Wang, Z., Hao, H. & Lu, Y., 2004. A three-phase soil model for simulating stress wave propagation due to blast loading. *International Journal for Numerical and Analytical Methods in Geomechanics*, 28(1), pp.33–56.

Wilkinson, C.R. & Anderson, J.G., 2003. An Introduction to Detonation and Blast for the Non-Specialist. *DSTO Weapons and Systems Division*, DSTO-TN-05.